

# MORPHOLOGICAL PROPERTIES OF NANOTEXTURED STRUCTURES PREPARED ON Si SURFACE

*Stanislav Jurečka<sup>1</sup>, Taketoshi Matsumoto<sup>2</sup>, Kentaro Imamura<sup>2</sup>, Hikaru Kobayashi<sup>2</sup>*

<sup>1</sup>*Institute of Aurel Stodola, University of Žilina, Nálepku 1390, 03101 Liptovský Mikuláš*

<sup>2</sup>*The Institute of Scientific and Industrial Research, Osaka University, CREST, Science and Technology Agency, Ibaraki, Osaka 567-0047, Japan*

*E-mail: jurecka@lm.uniza.sk*

*Received 30 April 2016; accepted 13 May 2016*

## 1. Introduction

Clean silicon surfaces show high spectral reflectance in the visible range of light wavelengths. Microtextured structures on Si surfaces are often used for increasing of light trapping in semiconductor devices, especially in the solar cells. Commonly used methods of surface structuring are based on anisotropic alkaline etching of silicon using KOH, NaOH, TMAH and isopropanol [1-5]. The reflectance of formed pyramidal structure decreases to 10 – 20 % [6]. Nanoporous Si structures with low reflectance are formed also by etching supported by catalytic activity of Au, Ag or Pt particles [7-8]. The thickness of porous Si layer reaches 500~1000 nm and causes problems in forming of the pn-junctions.

We prepared Si nanostructures with ultra-low spectral reflectance by using Pt meshassisted etching of Si. During the etching procedure a nanostructured layer is formed (Surface Structure Chemical Transfer method, SSCT) [9-11]. We also formed pyramidally etched Si structures by the SSCT method (PSSCT). We observe significant suppression of the spectral reflectance in both cases (SSCT and PSSCT). We examined the surface structures by the scanning electron microscope (SEM) and by the atomic force microscope (AFM). Properties of observed surface structures were analysed by the multifractal methods and by analysis of the SEM and AFM images in the 2D Fourier domain (2D FFT). Morphological properties of nanostructured surfaces are strongly related to the complexity of formed features revealed by the multifractal and 2D FFT analysis.

## 2. Experiments

Single crystalline p-type Si wafers were cleaned in 1.5 M KOH solutions at 80 ~ 85°C for 15 min. Pyramidal structures were formed by anisotropic etching in 0.25 M KOH and 0.6 M isopropanol solutions at 80°C for 20 min. During the SSCT etching the Si wafers were immersed in 15 wt% H<sub>2</sub>O<sub>2</sub> and 25 wt% HF solution at room temperature, and contacted with a platinum mesh. The prolongation of the SSCT etching procedure was 10, 20 and 30 s. SEM micrographs were measured by using a HITACHI S-2150 microscope and AFM scans were measured by the AIST-NT SmartSPM-1000 system.

## 3. Results and discussion

The surface morphology of observed structures is very complicated. The development of surface morphology during individual etching steps is described by the Fourier methods and multifractal analysis of the AFM and SEM images. Fig.1 shows AFM images of the SSCT

structure prepared on flat Si surface by various etching time - 10 s, 20 s and 30 s. We observe very intensive surface morphology modification during the SSCT etching. We transformed the AFM random surface height function by using two dimensional Fourier transformation. Information in the 2D FFT domain coded into grey color scale was analysed by statistical methods.

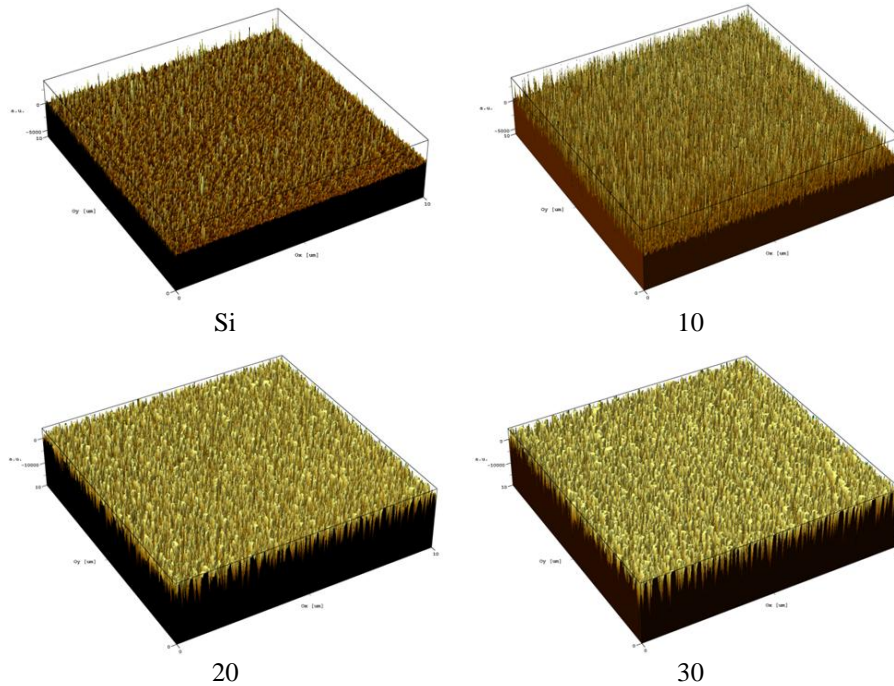


Fig.1: AFM images of the Si substrate and SSCT structure. SSCT etching time is 10, 20 and 30 s. Scanned area is  $10 \times 10 \mu\text{m}^2$ .

We computed histogram of the 2D FFT image values, see details in Fig.2. This analysis provides information about the surface features development with the prolongation of the SSCT etching time. With increasing etching time formation of small particle size fraction is emphasized as can be seen from the shift of the histogram centre.

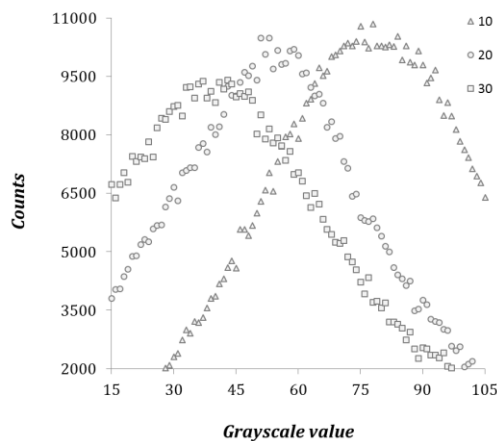


Fig.2: Histogram of values in a 2D FFT domain of the AFM SSCT structure etched for 10, 20, and 30 s.

The morphology of the nanostructured layers was examined at various magnifications of the SEM images in range from 100 to 40000. In Fig.3a-b SEM images of pyramidally textured and SSCT treated structures with the magnification of 2000 are shown. SSCT etching strongly influences the surface features as can be seen in Fig.3c, where the AFM image of the PSSCT surface area of  $10 \times 10 \mu\text{m}^2$  etched for 30 s is shown.

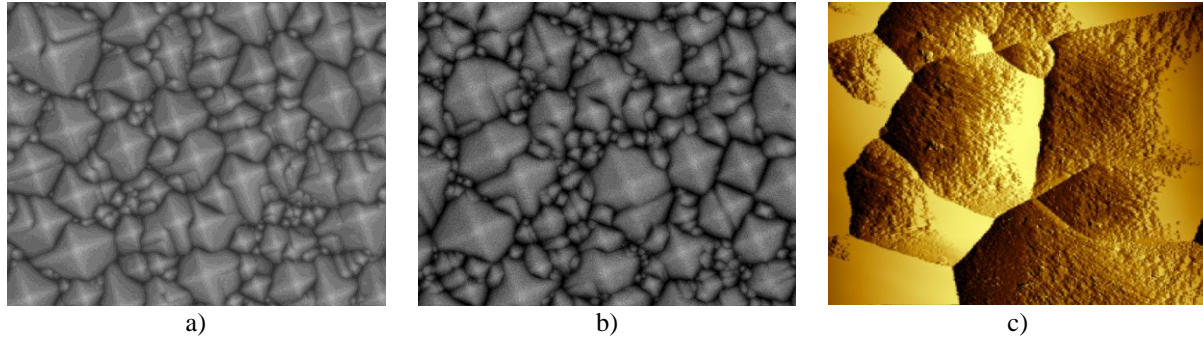


Fig.3: Scans of the PSSCT structure on Si. a) SEM, magnification 2000; b) SEM, magnification 2000; c) AFM, scanned area is  $10 \times 10 \mu\text{m}^2$ . SSCT etching time is a) 10 s, b) 20s, c) 30 s.

Morphological information from these structures was analysed by the multifractal detrended fluctuation analysis (MFDFA). MFDFA analysis provides information about scale invariant content in analysed surface structure [12-13]. Multifractal structures are described by the presence of spatial variations in the scale invariant structure and show a spectrum of power law exponents. In our approach the sequence of rows of the surface image are transformed into vector  $x(s)$ . This vector is detrended and the root-mean-square values (RMS) are evaluated. From the RMS analysis the singularity dimension  $D_h$  (called multifractal spectrum) and  $q$ -order singularity exponent  $h(q)$  are computed. Results of the MFDFA analysis of the SEM images with magnification 2000 (the development of the multifractal spectrum and the singularity exponent with the SSCT etching time) are shown in Fig.4 and Fig.5.

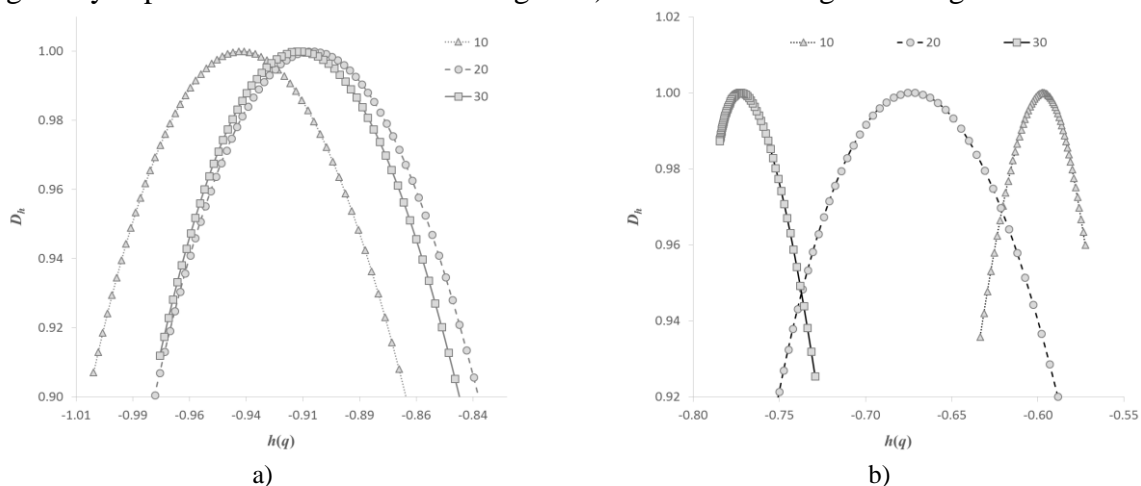


Fig.4. Results of the MFDFA analysis of SEM images of the SSCT structure: multifractal spectrum  $D_h$ . a) The SSCT morphology, b) the PSSCT morphology. SSCT etching time is 10 s, 20s and 30 s. SEM magnification is 2000.

Multifractal spectrum  $D_h$  of the SSCT structure is significantly shifted in the first 20 s of the SSCT etching as can be seen in Fig.4a. After this etching time the development of the

structure features are not so important. The surface morphology of the PSSCT structure develops also very intensively in the early stages of the SSCT etching followed by reaxation phase of the structure modification as indicated in the  $D_h$  behaviour illustrated in Fig.4b.

The symmetry of the  $D_h$  spectrum shows, that the multifractal SSCT structure contains fluctuations with both small and large magnitudes and the surface morphology stabilizes after the 20 s of etching. The development of the  $q$ -order singularity exponent  $h(q)$  with the prolongation of the SSCT etching is shown in Fig.5.

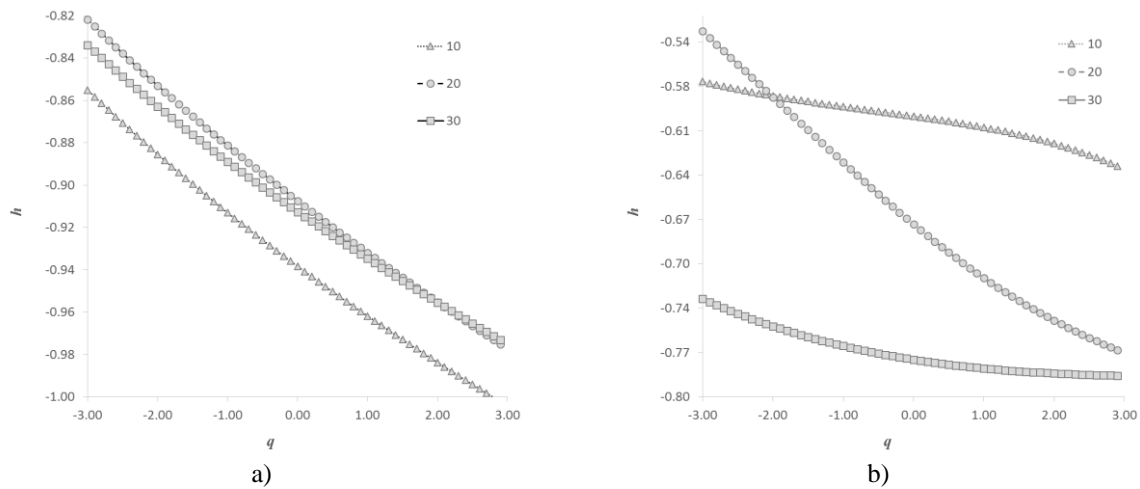


Fig.5: Results of the MFDFA analysis of SEM images of the SSCT structure:  $q$ -order singularity exponent  $h(q)$ . a) SSCT structure, b) PSSCT structure. SSCT etching time is 10 s, 20s and 30 s. SEM magnification is 2000.

We can see again the stabilization of the morphology development of the SSCT structures after the 20 s of etching from the  $h(q)$  behaviour in Fig.5a and the development of surface features with prolongation of etching time for PSSCT morphology in Fig.5b. The shape of the  $D_h$  spectra and singularity exponent  $h(q)$  curves in Fig.4b and Fig.5b indicate, that the multifractal PSSCT structure contains also fluctuations with small and large magnitudes and that various surface feature size fractions develop differently in comparison to the SSCT morphology.

Information from multifractal  $D_h$  and  $h(q)$  curves enables optimization of the SSCT etching procedure in order to reach required morphological properties, leading to suppression of the spectral reflectance values in a broad range of wavelengths.

## Acknowledgement

This work was partly supported by the Japan Society for the Promotion of Science, by projects ITMS 26220120046 and ITMS 26210120021, co-funded from EU sources and European Regional Development Fund and by project of Scientific Grant Agency of the Ministry of Education Slovak Republic and the Slovak Academy of Sciences VEGA 1/0076/15.

## References

- [1] P. K. Singh, R. Kumar, M. Lal, S. N. Singh, B. K. Das: *Sol. Energy Mater. Sol. Cells*, **70**, 103 (2001).
- [2] E. Vazsonyi, K. De Clercq, R. Einhaus, E. Van Kerschaver, K. Said, J. Poortmans, J. Szlufcik, J. Nijs: *Sol. Energy Mater. Sol. Cells*, **57**, 179 (1999).
- [3] P. Papet, O. Nichiporuk, A. Kaminski, Y. Rozier, J. Kraiem, J.-F. Lelievre, A. Chaumartin, A. Fave, M. Lemiti: *Sol. Energy Mater. Sol. Cells*, **90**, 2319 (2006).
- [4] H. Kim, S. Park, S. M. Kim, S. Kim, Y. D. Kim, S. J. Tark, D. Kim: *Current Appl. Phys.*, **13**, S34 (2013).
- [5] H. Angermann, J. Rappich, L. Korte, I. Sieber, E. Conrad, M. Schmidt, K. Hübener, J. Polte, J. Hauschild: *Applied Surface Science*, **254** (2008).
- [6] S. Jurečka, H. Angermann, H. Kobayashi, M. Takahashi, E. Pinčík: *Applied Surface Science*, **301**, 46 (2014).
- [7] J. Oh, H. Yuan, H. Branz: *Nature Nanotechnology*, **7**, 743 (2012).
- [8] K. Tsujino, M. Matsumura, Y. Nishimoto: *Sol. Energy Mater. Sol. Cells*, **90**, 100 (2006).
- [9] K. Imamura, F. C. Franco Jr, T. Matsumoto, H. Kobayashi: *Appl. Phys. Lett.*, **103**, 013110 (2013).
- [10] M. Takahashi, T. Fukushima, Y. Seino, W.-B. Kim, K. Imamura, H. Kobayashi: *J. Electrochem. Soc.*, **160**, H443 (2013).
- [11] D. Irishika, K. Imamura, H. Kobayashi: *Sol. Energy Mater. Sol. Cells*, **141**, 1 (2015).
- [12] J. W. Kantelhardt, S. A. Zschiegner, E. Koscielny-Bunde, S. Havlin, A. Bunde, H. E. Stanley: *Physica A* **316**, 87–11410.1016/S0378-4371(02)01383-3 (2002).
- [13] E. A. F. Ihlen., B. Vereijken: *J. Exp. Psychol. Gen.*, **139**, 436–46310.1037/a0019098 (2010).